

HIGH-POWER SOLID-STATE LASER: LETHALITY TESTING AND MODELING

R. P. Abbott, C. D. Boley, S. N. Fochs, L. A. Nattrass,
J. M. Parker, A. M. Rubenchik, J. A. Smith, and R. M. Yamamoto*
University of California
Lawrence Livermore National Laboratory
Livermore, CA 94551

ABSTRACT

We describe a high-power solid-state laser built in our laboratory and its applications to defense missions. We discuss selected target interaction experiments recently performed with this laser. These involve the irradiation of painted aluminum foils at a power of about 25 kW, in the presence of high-speed airflow. The spot sizes were large, covering the range 9-16 cm. Penetration was achieved within a few seconds, depending on the spot size. We present a numerical model which successfully describes the main experimental results.

1. INTRODUCTION

During the last several years, our laboratory has been developing high-power solid-state lasers for tactical battlefield applications (Yamamoto *et al.*, 2005). These lasers are based on a compact, flexible, single-aperture, mobile architecture that can be readily scaled to engagement-level powers (~ 100 kW). The lasing medium is a series of diode-pumped solid-state slabs, producing a beam at a wavelength of approximately 1 micron. During lasing operations, the waste heat is stored in the slabs. In a field device, the slabs would be rapidly interchanged with cool slabs, after several accumulated seconds of lasing.

Our most advanced laboratory laser has four ceramic YAG slabs (Soules *et al.*, 2005) pumped by diodes at a pulse repetition rate of 200 Hz. The aperture size is 10×10 cm². Figure 1 shows a view of this laser, and Fig. 2 shows details of the ceramic slabs. With this laser, routine operation has been achieved at a time-averaged power of about 25 kW (125 J per pulse) for several seconds. Since the laser has a pulsed format, this is the power averaged over an interval longer than several pulses. At 200 Hz, an individual pulse arrives every 5 ms. The pulse length is about 0.5 ms, giving a duty factor of 10%. The time-averaged power is the same as the equivalent CW power.

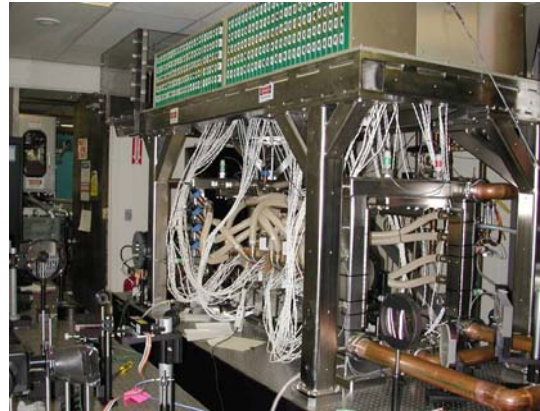


Fig. 1. Laboratory view of 25 kW diode-pumped laser.



Fig. 2. Ceramic YAG slabs. The dimensions of the slabs are $10 \times 10 \times 2$ cm³.

We have investigated the lethality of this laser, also called a Tailored Aperture Ceramic Laser (TACL), against a variety of battlefield targets. Here we deal with thin sheets of painted aluminum, subjected to high-speed airflow. The temperature of the back surface was recorded as a function of time. The beam was found to penetrate a target within a few seconds, depending on the spot size.

Report Documentation Page				Form Approved OMB No. 0704-0188	
Public reporting burden for the collection of information is estimated to average 1 hour per response, including the time for reviewing instructions, searching existing data sources, gathering and maintaining the data needed, and completing and reviewing the collection of information. Send comments regarding this burden estimate or any other aspect of this collection of information, including suggestions for reducing this burden, to Washington Headquarters Services, Directorate for Information Operations and Reports, 1215 Jefferson Davis Highway, Suite 1204, Arlington VA 22202-4302. Respondents should be aware that notwithstanding any other provision of law, no person shall be subject to a penalty for failing to comply with a collection of information if it does not display a currently valid OMB control number.					
1. REPORT DATE 01 NOV 2006		2. REPORT TYPE N/A		3. DATES COVERED -	
4. TITLE AND SUBTITLE High-Power Solid-State Laser: Lethality Testing And Modeling				5a. CONTRACT NUMBER	
				5b. GRANT NUMBER	
				5c. PROGRAM ELEMENT NUMBER	
6. AUTHOR(S)				5d. PROJECT NUMBER	
				5e. TASK NUMBER	
				5f. WORK UNIT NUMBER	
7. PERFORMING ORGANIZATION NAME(S) AND ADDRESS(ES) University of California Lawrence Livermore National Laboratory Livermore, CA 94551				8. PERFORMING ORGANIZATION REPORT NUMBER	
9. SPONSORING/MONITORING AGENCY NAME(S) AND ADDRESS(ES)				10. SPONSOR/MONITOR'S ACRONYM(S)	
				11. SPONSOR/MONITOR'S REPORT NUMBER(S)	
12. DISTRIBUTION/AVAILABILITY STATEMENT Approved for public release, distribution unlimited					
13. SUPPLEMENTARY NOTES See also ADM002075., The original document contains color images.					
14. ABSTRACT					
15. SUBJECT TERMS					
16. SECURITY CLASSIFICATION OF:			17. LIMITATION OF ABSTRACT UU	18. NUMBER OF PAGES 5	19a. NAME OF RESPONSIBLE PERSON
a. REPORT unclassified	b. ABSTRACT unclassified	c. THIS PAGE unclassified			

This occurred well before the back surface reached the melting temperature.

We have developed a simple model of these experiments. We show that it quantitatively reproduces the main experimental results. Most notable of these is the linear increase of temperature with time, up to the moment of material failure.

2. TARGET INTERACTIONS: EXPERIMENT

The experiments described here involved irradiation of a thin (0.18 cm) sheet of aluminum. The aluminum was painted on the irradiated side with a black paint. The sheet was situated near a nozzle which maintained air flow at about 100 m/s, or about Mach 0.3. The primary lethality diagnostic was a thermocouple attached to the back face of the aluminum, near the center of the beam footprint. The spot size was approximately square. The experimental setup with a penetrated target in place, just after laser interaction, is shown in Fig. 3.

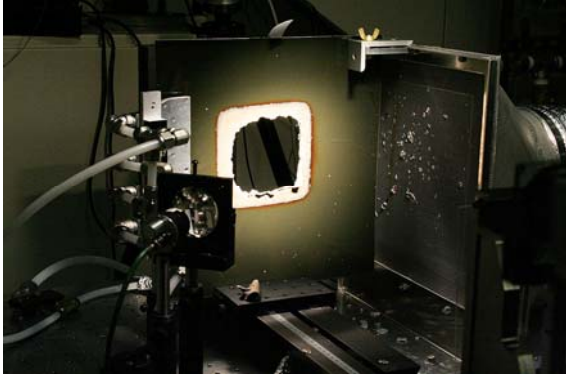


Fig. 3. Experimental setup, just after irradiation of a coupon (13x13 cm² spot size). To the left of the target is the blower assembly (partially concealed). To the right is the suction assembly. Note coupon pieces on the screen. The laser is beyond the field of view, to the front and right.

The test results for the three coupon tests are summarized in Table 1, which gives the spot sizes, penetration times, and penetration temperatures. The terms “penetration time” and “penetration temperature” refer to the point at which the thermocouple reading suddenly begins to fall. Before this point, it rises almost linearly to the maximum. Actual temperature traces are shown and

Table 1. Parameters of the Experimental Runs

Run	Spot Size (cm ²)	Penetration Time (s)	Penetration T (C)
A	9.1 x 8.8	0.8	390
B	13 x 13	2.4	550
C	15.2 x 16.5	3.6	580

discussed in the next section. The penetration time increases about linearly with spot area.

The penetration of a 13x13 cm² coupon is dramatically illustrated in the five frames of Fig. 4. Note that the target first bulges outward, toward the beam. Then metal pieces, of size exceeding a cm, begin to break off. Finally, a large central hole is formed.

The most interesting result of our experiment is that the target breaks well below the melting temperature (660 C). This can be explained in the following way. When the aluminum is heated up to about 400 C, it softens and the strength nearly vanishes. At the same time, the wind stream produces, according to Bernoulli’s law, a pressure decrease $\Delta p = -\rho u^2 / 2$ near the external target surface. This pressure difference causes the outward bulge seen in the first frame of Fig. 4. The target then breaks. Among the collected debris, we found large pieces of unmelted material. The fact that the target breaks at a temperature $T_s < T_m$ reduces the penetration time by a factor $(T_m - T_s)/T_m \sim 0.4$. Equivalently, for a given penetration time, the required laser power is reduced by this factor.

3. TARGET INTERACTIONS: MODELING

To model these experiments, the most important consideration is the high thermal conductivity of aluminum, which corresponds to a thermal diffusivity of about 0.85 cm²/s. This is an average value between room temperature and melting temperature. As a result, the time required for heat to conduct across the aluminum foil is very small (about 10 ms) compared to the lasing time. Thus the temperature profile across the coupon width is essentially flat. In this picture, the laser fills up the volume beneath the irradiated spot with heat, until the temperature reaches a point at which the material strength falls to zero. This picture is complicated somewhat by lateral heat conduction. However, this phenomenon is not too important for the large spot sizes of interest. The

conduction distance during the lasing time is a few cm, which is tolerably small compared to the spot sizes.

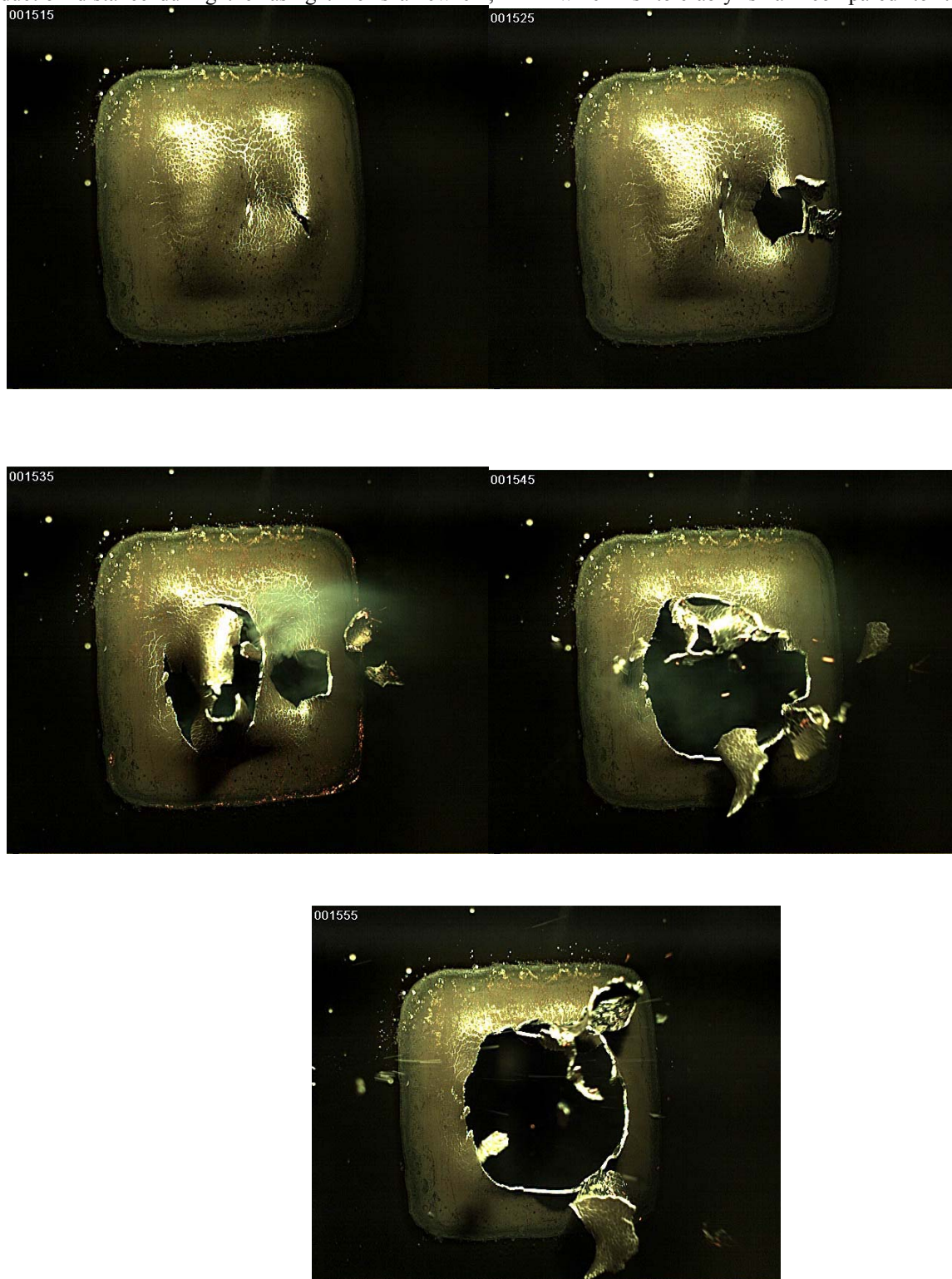


Fig. 4. Stages in the penetration of a coupon. The beam ($13 \times 13 \text{ cm}^2$ spot size) is directed into the figures. The photographs are taken during intervals between pulses. The time between frames is 167 ms. Note the initial outward bulge, followed by the removal of macroscopic pieces.

Another complication is the role of paint, which we discuss below. Finally, we neglect wind cooling, which is small compared to the laser power.

Putting this information together, we see that the material temperature T satisfies

$$Ah\rho C \frac{dT}{dt} = \alpha P, \quad (1)$$

where A is the spot area, h is the foil thickness, ρ is the material density, and C is the specific heat. Also P is the time-averaged laser power, and α is the optical absorptivity of the coupon. The left-hand side of this equation gives the rate of increase of heat beneath the spot, and the right-hand side gives the power absorbed. Since the density and heat capacity change with temperature, we use values midway between room temperature and melting temperature. These are $\rho = 2.54 \text{ g/cm}^3$ and $C = 1.08 \text{ J/(g K)}$. The absorptivity of aluminum at room temperature is of order 10% or less, depending on the surface finishing. However, it increases with temperature, reaching about 25% at the melting temperature (Boley and Rubenchik, 2006a). Paint is a complicated material, but here we shall suppose that it serves only to increase the effective absorptivity. For the black paint of these experiments, we take $\alpha \sim 0.8$. Measurements during the experiments indicate that the absorptivity does not decrease up to breakthrough. They also indicate that the paint survives up to this point.

According to the model, the temperature increases linearly with time. For a given laser power, it decreases linearly with spot area. In the absence of detailed information about material failure, we extend the solutions to the melting point of aluminum.

Temperature traces for both experiment and model are shown in Fig. 5. In all three cases, the model results agree very well with experiment, until the moment of coupon failure. If we supposed that failure occurred at a particular temperature, then the model penetration time would increase linearly with spot area, as seen in experiment. Of course the measured failure temperatures vary somewhat for the various cases. There may be some uncertainty near the point of failure. For example, if the coupon began to fail near the edge rather than at the center, then the thermocouple would have remained attached to a dislodged piece and the measured temperature would have continued to rise.

Our model can be supplemented to handle a number of additional effects, including heat

conduction (in both longitudinal and transverse directions), temperature-dependent material properties, a more detailed paint model, and wind effects (Boley and Rubenchik, 2006b). For these experiments, however, the more sophisticated model yields overall results nearly identical to those presented here. Hence the approximations made above appear to be realistic.

CONCLUSIONS

We have described target experiments performed with a high-power solid-state laser built in our laboratory. The experiments involved the irradiation of painted aluminum foils at a power of about 25 kW, with large spot sizes (9 – 16 cm). The foils were penetrated within a few seconds. It is noteworthy that penetration occurred before the target melted, and that macroscopic pieces (size up to a few cm) were removed. The phenomena can be understood on the basis of a numerical model.

ACKNOWLEDGMENTS

This work was performed under the auspices of the U.S. Department of Energy by the University of California, Lawrence Livermore National Laboratory, under Contract No. W-7405-ENG-48.

REFERENCES

- Boley, C. D., and Rubenchik, A. M., 2006a: Lethality of a High-Power Solid-State Laser, Ninth Annual Directed Energy Symposium, November 2006, Albuquerque, NM.
- Boley, C. D., and Rubenchik, A. M., 2006b: Modeling of Antimortar Lethality by a Solid-State Heat-Capacity Laser, *J. Directed Energy* (in press).
- Soules, T. F., et al., 2005: Ceramic Nd:YAG – Current Material of Choice for SSHCL, Eighth Annual Directed Energy Symposium, November 14-18, 2005, Lihue, HI.
- Yamamoto, R. M., et al., 2005: The Solid-State Heat-Capacity Laser (SSHCL) Program at LLNL, Proceedings of the Eighth Annual Directed Energy Symposium, November 14-18, 2005, Lihue, HI.

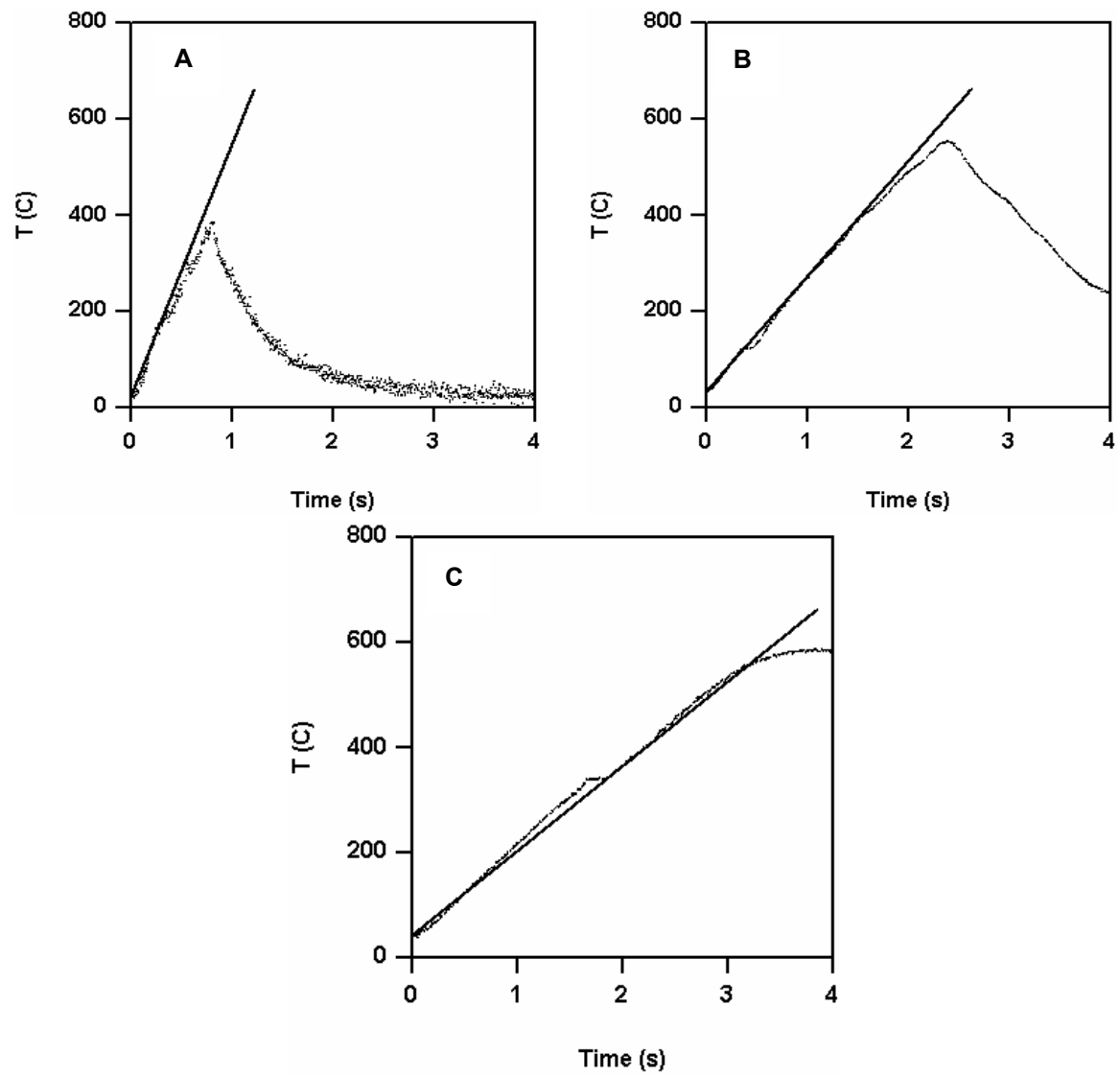


Fig. 5. Temperature versus time for the three experiments. The dotted lines give experimental points, while the solid lines give model results.